Rigid Macrocyclic Triamides as Anion Receptors: Anion-Dependent Binding Stoichiometries and [1]H Chemical Shift Changes

Kihang Choi and Andrew D. Hamilton*

Contribution from the Department of Chemistry, Yale University, New Haven, Connecticut 06520

Received February 7, 2003; E-mail: andrew.hamilton@yale.edu

Abstract: The cyclic triamide of 3′-amino-3-biphenylcarboxlic acid is readily synthesized in a stepwise manner and represents a novel class of anion receptors with a large central cavity. This macrocycle binds more strongly to tetrahedral anions than spherical or planar anions in organic solvents. The binding stoichiometries for anions with symmetrical charge distribution depend on the solvent polarity, while tetrahedral p-tosylate binds to the macrocycle with 1:1 stoichiometry in all solvents studied. The ^{1}H NMR chemical shift changes of the protons lining the interior of the macrocycle's central cavity also depend on the geometry of the bound anion. The importance of the convergent array of hydrogen bond donors for anion binding by the macrocycle was confirmed by control studies with an acyclic triamide and a macrocycle with intramolecular hydrogen bonds.

Introduction

Macrocycles have been widely used in molecular recognition studies, and many synthetic receptors for biologically and environmentally important small molecules have been constructed on the basis of such cyclic molecules as crown and azacrown ethers, calixarenes, and porphyrins.[1] Macrocyclic structures are particularly effective at reducing conformational flexibility and in preorganizing ligand binding elements relative to their acyclic analogues. The convergent arrangement of binding groups within a constrained macrocyclic scaffold provides an effective microenvironment for the recognition of small ions or molecules. In particular, the controlled positioning of binding groups within a macrocycle allows geometrical and size discrimination in the recognition of a small substrate.

Symmetrical macrocycles are usually synthesized by condensation of repeating units (monomers) followed by cyclization, often in a single step (Scheme 1). Efficient one-pot synthesis of large macrocycles with multiple functional groups, like calixarenes or porphyrins, has led to the widespread use of these derivatives in molecular recognition studies. However, their ease of synthesis creates serious difficulties when less symmetrical or more functionalized derivatives are required. An advantage of using conformationally rigid macrocycles as artificial receptors is that potential binding elements can be constrained to match the pattern of functional groups on the target molecule.

**Scheme 1.** Two Strategies for Macrocyclic Receptor Synthesis
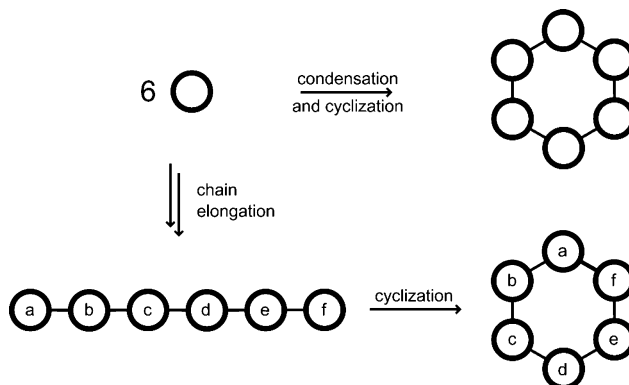
In this way an unsymmetrical receptor can be designed with the optimal positioning of binding groups to bind strongly and selectively to an unsymmetrical substrate. Even in the case of symmetrical substrates, more complex receptors may be required for sensing or other advanced applications. Symmetrical macrocycles such as calixarenes and porphyrins have limited use in the formation of unsymmetrically functionalized receptors. Desymmetrization of a symmetrical molecule through differential modification of several functional groups tends to give product mixtures, including regioisomers that are difficult to separate. This is especially the case with large rigid macrocycles where the kinetic influence of one functional group on another is unlikely. These difficulties lead to low yields and arduous purification steps in the preparation of unsymmetrical receptors by desymmetrization of symmetrical macrocyclic scaffolds.

An alternative approach in macrocycle synthesis is cyclization of a linear precursor that is assembled from monomers in a

(1) Crown and azacrown ethers: (a) Izatt, R. M.; Bradshaw, J. S.; Nielsen, S. A.; Lamb, J. D.; Christensen, J. J. *Chem. Rev.* **1985**, *85*, 271−339. (b) Izatt, R. M.; Pawlak, K.; Bradshaw, J. S. *Chem. Rev.* **1995**, *95*, 2529−2586. Cyclodextrins: (c) Szejtli, J. *Chem. Rev.* **1998**, *98*, 1743−1753. Calixarenes: (d) Ikeda, A.; Shinkai, S. *Chem. Rev.* **1997**, *97*, 1713−1734. Porphyrins: (e) Ogoshi, H.; Mizutani, T. *Curr. Opin. Chem. Biol.* **1999**, *3*, 736−739. Calixpyrroles: (f) Gale, P. A.; Sessler, J. L.; Kral, V. *Chem. Commun.* **1998**, 1−8.

stepwise manner. This stepwise synthesis usually consists of a repeated cycle of reactions leading to an appropriate linear oligomer that is then cyclized in the final step (Scheme 1). Both symmetrical and unsymmetrical macrocycles can be synthesized using monomers with different functional groups. Several stepwise syntheses have been reported recently[2] of large macrocycles containing an interior cavity with multiple groups, which have then been successfully used as synthetic receptors for small molecules.

As part of our work on anion recognition by directed hydrogen-bonding interactions, we sought a novel class of macrocyclic receptors that contained a constrained binding site but could be prepared in a facile stepwise manner.[3] We now report in full on the design of macrocyclic receptor **1** based on the cyclic trimerization of 3′-amino-3-carboxybiphenyl subunits.

1a R = CO₂Et
b R = NHBoc
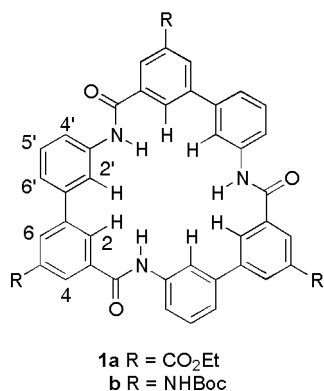
Macrocycle **1** has a rigid trigonal structure in which three hydrogen-bonding amide groups are projected into the central cavity. This convergent arrangement of dipoles enables the macrocycle to bind anions with size and shape selectivity and in a manner that is dependent on the anion and the polarity of the solvent. The stepwise modular synthesis of the macrocycle makes the modifications inside and outside the cavity relatively straightforward and allows us to demonstrate the importance of convergent hydrogen bonding in anion recognition.

Result and Discussion

Design and Synthesis. The cyclic trimer of 3′-aminobiphenyl-3-carboxylic acid **1** has been designed as a novel macrocyclic receptor for tetrahedral anions. This compound has size and rigidity comparable to those of other macrocycles such as porphyrins, calixarenes, and calixpyrroles. There are only nine rotatable dihedral angles and no sp³-hybridized atoms in this 24-membered ring system. The small number of flexible bonds and the substitution pattern of the biphenyl monomer suggest that cyclization should be favorable and that yields of the macrocycle might be reasonable. The rigid aromatic rings not only reduce conformational flexibility but also provide the
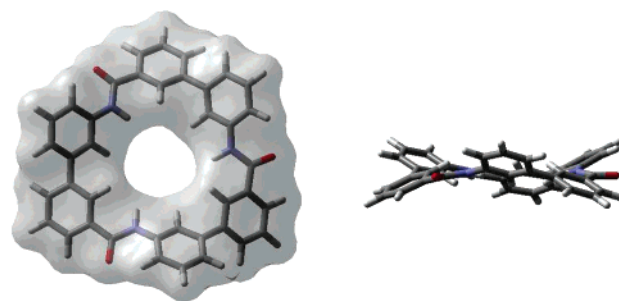

Figure 1. Lowest energy conformation of the cyclic trimer of 3′-aminobiphenyl-3-carboxylic acid. A conformational search was carried out using MacroModel (version 6.5). The 2000 separate search steps were followed by energy minimization using the MM2* force field and CHCl₃ solvation parameters. On the left side, the macrocycle is shown together with its solvent-accessible surface (Connolly surface calculated with 1.4 Å probe radius). Atoms are colored following the CPK color code (C, gray; H, white; O, red; N, blue).

macrocycle with potential modification sites for the introduction of additional receptor functions.

To obtain a detailed picture of the macrocycle structure, a Monte Carlo conformational search was performed using MacroModel.[4] Six conformers were found within 3 kcal/mol energy of the lowest energy conformation (the number of conformers increases to 16 if the molecular symmetry is not considered). The lowest energy conformer (Figure 1) has C_3 symmetry with three carbonyl oxygen atoms projecting outside and three amide protons projecting into the center of the macrocycle. This orientation of amide bonds is likely due to steric effects with the small hydrogen atoms occupying the sterically congested cavity while the bulkier oxygen atoms are placed outside the ring. The dimensions of the molecule are about 15 Å × 15 Å and similar to those of tetraphenylporphyrins. There is a hole approximately 5 Å in diameter and lined only with hydrogen atoms (three from the amides and six from the aryl groups) in the center. The six phenyl rings are tilted up and down in an alternating sequence, and the distance between two meta positions of the adjacent biaryl monomers corresponds to approximately 12 Å. The torsion angle between the two phenyl rings of each biphenyl system is approximately 45°, which is similar to that of a simple biphenyl in its lowest energy conformation.[5] In the other low-energy conformers of the macrocycle, alternating sequences of the phenyl rings and orientations of amide bonds are changed slightly.

The macrocycle synthesis began with the preparation of the biaryl monomers (Scheme 2). The first synthesized monomer was 5-(ethoxylcarbonyl)-3′-nitro-3-biphenylcarboxylic acid **3**, prepared from 3-nitrophenylboronic acid and 1-iodo-3,5-dimethylbenzene. After the Suzuki coupling reaction, potassium permanganate oxidation of **2** at the benzylic positions provided the corresponding isophthalic acid. Fischer esterification of the isophthalic acid gave the corresponding diethyl ester, which in turn was hydrolyzed to monoester **3** in a statistical yield. A more efficient route to a similar biaryl monomer was devised subsequently, starting from commercially available 5-nitroisophthalic acid monomethyl ester. After catalytic hydrogenation

(2) (a) Ishida, H.; Suga, M.; Donowaki, K.; Ohkubo, K. *J. Org. Chem.* **1995**, *60*, 5374−5375. (b) Rasmussen, P. H.; Rebek, J., Jr. *Tetrahedron Lett.* **1999**, *40*, 3511−3514. (c) Kubik, S.; Goddard, R.; Kirchner, R.; Nolting, D.; Seidel, J. *Angew. Chem., Int. Ed.* **2001**, *40*, 2648−2651. (d) Burke, S. D.; Zhao, Q. *J. Org. Chem.* **2000**, *65*, 1489−1500. (e) Burke, S. D.; Zhao, Q.; Schuster, M. C.; Kiessling, L. L. *J. Am. Chem. Soc.* **2000**, *122*, 4518−4519. (f) Campbell, J. E.; Englund, E. E.; Burke, S. D. *Org. Lett.* **2002**, *4*, 2273−2275. (g) Lowik, D. W. P. M.; Lowe, C. R. *Tetrahedron Lett.* **2000**, *41*, 1837−1840. (h) Yang, D.; Qu, J.; Li, W.; Zhang, Y. H.; Ren, Y.; Wang, D. P.; Wu, Y. D. *J. Am. Chem. Soc.* **2002**, *124*, 12410−12411.
(3) Choi, K.; Hamilton, A. D. *J. Am. Chem. Soc.* **2001**, *123*, 2456−2457.

(4) Mohamadi, F.; Richards, N. G.; Guida, W. C.; Liskamp, R.; Lipton, M.; Caufield, C.; Chang, G.; Hendrickson, T.; Still, W. C. *J. Comput. Chem.* **1990**, *11*, 440−467.
(5) (a) Almenningen, A.; Bastiansen, O.; Fernholt, F.; Cyvin, B. N.; Cyvin, S. J.; Samdal, S. *J. Mol. Struct.* **1985**, *128*, 59−76. (b) Arulmozhiraja, S.; Fujii, T. *J. Chem. Phys.* **2001**, *115*, 10589−10594.

Scheme 2. Synthesis of Biphenyl Monomers[a]
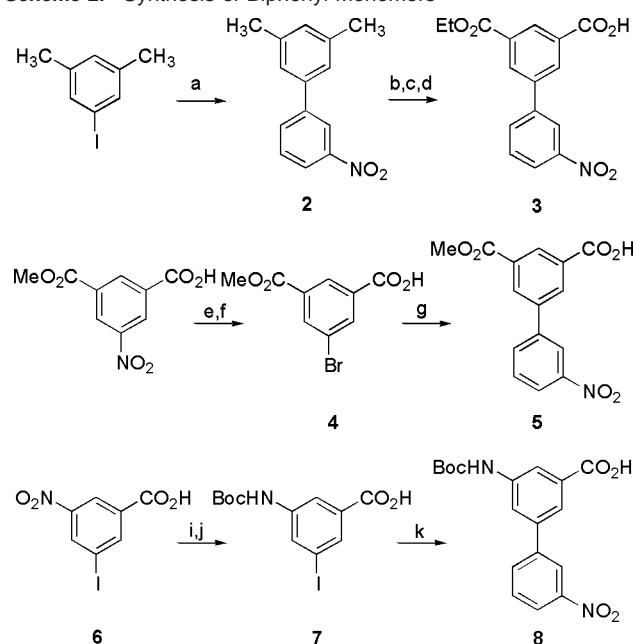
[a] (a) $m\text{-}NO_2\text{-}C_6H_4B(OH)_2$, $Pd(Ph_3P)_4$, PPh_3, Na_2CO_3, 94%; (b) $KMnO_4$, H_2O, pyridine; (c) $p\text{-}TsOH$, EtOH; (d) 1 equiv of NaOH, H_2O, EtOH, THF, 52% from **2**; (e) H_2, Pd/C; (f) $NaNO_2$, HBr, H_2O, CuBr, 95%; (g) $m\text{-}NO_2\text{-}C_6H_4B(OH)_2$, $Pd(OAc)_2$, Cs_2CO_3, 81%; (h) I_2, H_2SO_4, 93%; (i) $(NH_4)_2\text{-}Fe(SO_4)_2$; (j) $(Boc)_2O$, KOH, H_2O, 1,4-dioxane, 80% from **6**; (k) $m\text{-}NO_2\text{-}C_6H_4B(OH)_2$, $Pd(OAc)_2$, Na_2CO_3, 83%.

of the nitro group, the aniline product was treated with $NaNO_2$ in hydrobromic acid to generate the corresponding diazonium salt. Sandmeyer reaction of the diazonium compound afforded 5-bromoisophthalic acid monomethyl ester **4**, which was then coupled with 3-nitrophenylboronic acid to generate biaryl monomer **5**. Another biaryl monomer that has a Boc-protected amine group instead of a carboxylic ester was also prepared. The nitro group of **6** could be efficiently converted to the corresponding amine using $(NH_4)_2Fe(SO_4)_2$ and was then protected as its Boc carbamate **7**. A Boc group was selected as the protecting group because of its facile deprotection reaction and its solubilizing effect on the intermediate oligomers and macrocycles in organic solvents. Biaryl monomer **8** was obtained in a good yield by coupling aryl iodide **7** with 3-nitrophenylboronic acid using $Pd(OAc)_2$ as a catalyst with no added ligands.

The isophthalic acid monoesters were converted to the corresponding acid chloride or used directly as an acid component in the synthesis of biaryl dimers **9**. The amine component was prepared by protection of the carboxylic acids as their 2-(trimethylsilyl)ethyl esters (using DCC in the presence of an acylation catalyst, DMAP) and reduction of the nitro groups by catalytic hydrogenation (Scheme 3). BOP-Cl was used as a coupling reagent to generate biaryl dimers and trimers in reasonable yields (>70%). Carboxyl group deprotection and nitro group reduction of the trimers were carried out under mild conditions to give the linear precursors ready for macrocyclization, which proceeded under high dilution conditions with the same coupling reagent in 40−60% yields. The structure of the cyclization product was initially confirmed by its simplified NMR spectrum (relative to the acyclic trimer) and finally by mass spectrometry and elemental analysis.

Anion Binding. 1:1 Complexation. Macrocycle **1** has three amide groups projected into the center of the cavity. This

Scheme 3. Synthesis of Macrocycle **1**[a]
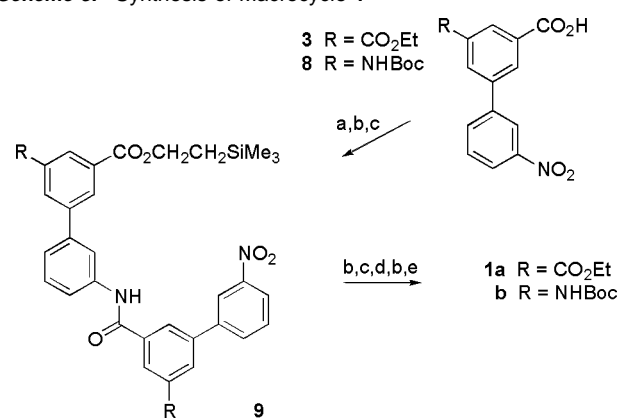
[a] (a) $Me_3SiCH_2CH_2OH$, DCC, DMAP, CH_2Cl_2; (b) H_2, Pd−C; (c) **3** or **8**, BOP−Cl, DIEA; (d) TBAF; (e) BOP−Cl, DIEA.
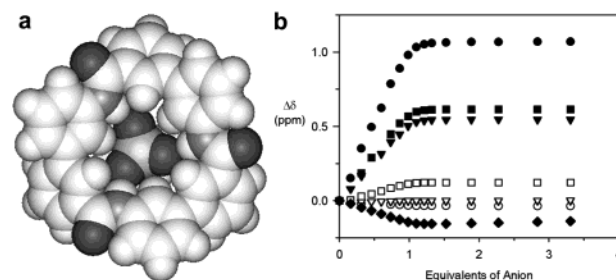

Figure 2. (a) Calculated structure of the 1:1 complex between macrocycle **1** and *p*-tosylate anion. The lowest energy conformation of the macrocycle was used as an initial structure for the calculation with the MM2 force field. R groups are omitted for clarity. (b) Change in ^1H chemical shift of **1b** with increasing *p*-TsO$^-$ concentration in 2% DMSO-d_6/CDCl$_3$ (●, amide NH; ■, C2′H; ▼, C2H; □, C4′H; ▽, C4H; ○, C6H; ◆, BocNH). C5′H and C6′H, which overlap each other, showed little change (∼0.03 ppm). [**1b**] = 0.75 mM. Association constant $K_a = 2.1 \times 10^5$ M^{-1}.

convergent and rigid arrangement of dipoles could allow the macrocycle to bind small molecules with hydrogen bond acceptors such as anions.[6] The size of the cavity and skewed arrangement of three amide protons are well-matched to the sizes and shapes of tetrahedral oxyanions such as sulfate and phosphate. A calculated structure for the 1:1 complex between macrocycle **1** and the *p*-tosylate anion shows that there are no significant changes in the macrocycle conformation after anion binding (Figure 2a). The complex retains C_3 symmetry with a minor tilting of the amide groups toward the bound anion, leading to an increase in the torsion angle of 5° between the two phenyl rings of each monomer. The hydrogen bond distance between the amide proton and the anion oxygen atom is 2.0 Å, and the N−H···O bond angle is 178°.

To determine the anion binding properties of the macrocycle, NMR titration experiments were performed. Macrocycle **1b**, which has Boc groups instead of carboxylic esters, has better solubility than **1a** and can be dissolved in CDCl$_3$ at millimolar concentrations. To dissolve **1a**, however, a small amount of a more polar solvent like DMSO-d_6 had to be added to CDCl$_3$. Macrocycle ^1H chemical shifts are independent of concentration over the range from 0.1 to 5.0 mM in 2% DMSO-d_6/CDCl$_3$ at

(6) Recent reviews of synthetic anion receptors: (a) *Supramolecular Chemistry of Anions*; Biaci, A., Bowman-James, K., Carcia-Espana, E., Eds.; VCH: Weinheim, Germany, 1997. (b) Beer, P. D.; Gale, P. A. *Angew. Chem., Int. Ed.* **2001**, *40*, 487−516. (c) Antonisse, M. M. G.; Reinhoudt, D. N. *Chem. Commun.* **1998**, 443−448. (d) Schmidtchen, F. P.; Berger, M. *Chem. Rev.* **1997**, *97*, 1609−1646.

296 K, thereby excluding possible aggregation effects. All association constant measurements were performed using 0.5– 1.0 mM macrocycle solutions, and ^{1}H NMR signals of the macrocycles were assigned using correlation spectroscopy (COSY) and nuclear Overhauser effect spectroscopy (NOESY) experiments. Several anions were tested for binding to the macrocycle, and changes in the chemical shifts were monitored as a function of anion concentration. To minimize possible effects of ion-pair formation and to take advantage of their good solubilities in organic solvents, tetrabutylammonium (TBA) salts were used in the titration experiments.

Titration of **1** with the *p*-tosylate anion gave 1:1 binding isotherms for the amide and aryl protons (Figure 2b), and the 1:1 binding ratio was confirmed by a Job's plot.[7] The large chemical shift changes of the NH, C2H, and C2′H protons clearly indicate that anion binding occurs inside the central cavity. The amide proton signal showed the largest downfield shifts presumably due to direct hydrogen bond formation between the amide NH and the oxygen atoms of the bound anion. The complexation-induced chemical shift changes ($\Delta\delta$) of the aryl protons projecting into the central cavity (C2H, C2′H) are much larger than those of the externally directed protons, indicating a deshielding effect from the anion positioned close to these protons. The intermolecular hydrogen bond formation does not seem to have significant through-bond electronic effects on C2H and C2′H because the C4H and C4′H protons, which are connected to the amide proton through the same numbers of chemical bonds, showed only small chemical shift changes.

Interestingly, the BocNH proton also showed chemical shift changes as a function of anion concentration despite being distant from the anion binding site inside the macrocycle. The upfield shift to 1 equiv addition of the anion ($\Delta\delta \approx 0.15$ ppm) is presumably caused by increased electron density on the biphenyl C5 position as a result of anion binding. Above 1.0 equiv, a small downfield shift of the BocNH resonance was observed, indicating the formation of weak hydrogen bonds with excess anion. The aryl protons of *p*-TsO$^-$ were shifted upfield by ~0.3 ppm upon complexation presumably because of the ring current effect of the macrocycle. Macrocycles **1a** and **1b** showed similar binding affinities, indicating that the overall anion binding properties are not affected significantly by the functional groups outside the central cavity.

Anion Binding. 2:1 Complexation. Anions other than *p*-TsO$^-$ showed more complex binding behavior that was characterized by initial upfield shifts (especially of the amide protons) up to 0.5 equiv addition of anionic substrate. Above 0.5 equiv, the direction of the shift changed to downfield (Figure 3). This type of binding isotherm is indicative of two equilibria,

$$\text{M} + \text{I} \overset{K_1}{\rightleftharpoons} \text{MI}$$

and

$$\text{MI} + \text{M} \overset{K_2}{\rightleftharpoons} \text{M}_2\text{I}$$
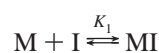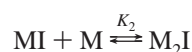
where M is macrocycle and I is ion. Since the macrocycle is in excess at the beginning of the titration, the first complex formed

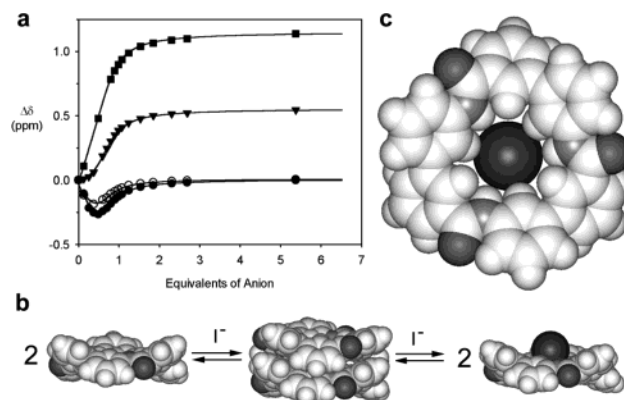(7) Conners, K. A. *Binding Constants*; John Wiley: New York, 1987.

Figure 3. (a) Change in ^{1}H chemical shift of **1b** with increasing I$^-$ concentration (●, amide NH; ■, C2′H; ▼, C2H; ○, C6H). The data were curve-fitted to the multiple-equilibrium model involving 1:1 and 2:1 complexes of the macrocycle with I$^-$. K_1 and K_2 were determined as 1.2 × 10^5 and 9.0 × 10^3 M^{-1}, respectively. Conditions as in Figure 2a were used. (b) Multiple-equilibrium model used for the curve fitting. M$_2$I and MI structures were calculated using the MM2 force field. The iodide anion of the M$_2$I complex is located between two macrocycles. (c) Bottom view of the 1:1 complex.

is M$_2$I, which is present at the highest concentrations near 0.5 equiv of anion. As the anion concentration increases, the equilibrium shifts to the MI complex and reaches saturation point toward the end of the titration.

The binding isotherms of the amide and aryl protons fit to a model of M$_2$I and MI complex formation, and the association constants of each equilibrium step could be obtained.[8,9] Spherical halide and planar nitrate ions showed this mode of binding. The even distribution of charge on these anions allows them to bind to two equivalent macrocycles in a 2:1 sandwich complex (Figure 3b). This accounts for the upfield shifts of the macro-cycle protons in the M$_2$I complex from ring current effects in the π-stacked structures. The NH, C6H, C4H, and C4′H protons were shifted upfield upon 2:1 complex formation. Whereas in the 1:1 complex the C2′H and C2H protons exhibited large downfield shifts, the other protons showed little change compared to those in the free macrocycle. The small change in the amide NH proton upon 1:1 complexation with I$^-$ is in contrast to the expected effect of a hydrogen bond with the anion. This is probably a result of the distance and/or the angle of the hydrogen bond being forced outside the optimum range by the mismatched size and shape of the anion.[10]

When the TBA salts of HSO$_4^-$ or H$_2$PO$_4^-$ were added to **1** in 2% DMSO-d_6/CDCl$_3$, second and third sets of ^{1}H NMR signals were observed depending on the concentration of the anion (Figure 4). The new sets of signals retained the simplicity found in the signals of the free macrocycle, suggesting sym-metrical structures for the new species. The intensities of the second set of signals, presumably from the M$_2$I complex, increased as the anion was added up to 0.5 equiv, while those of the free macrocycle decreased below the detection limit. Above 0.5 equiv, a third set of proton signals from the MI complex appeared while the second set of signals diminished

(8) The chemical shift data were analyzed using EQNMR. Hynes, M. J. *J. Chem. Soc., Dalton Trans.* **1993**, 311–312.

(9) For other anion receptors forming 2:1 complexes, see the following: Hossain, M. A.; Llinares, J. M.; Powell, D.; Bowman-James, K. *Inorg. Chem.* **2001**, *40*, 2936–2937 and ref 2c.

(10) Macrocyclic receptors for anions showing complexation-induced upfield shifts of amide NH proton signals have been reported recently. See ref 2h.
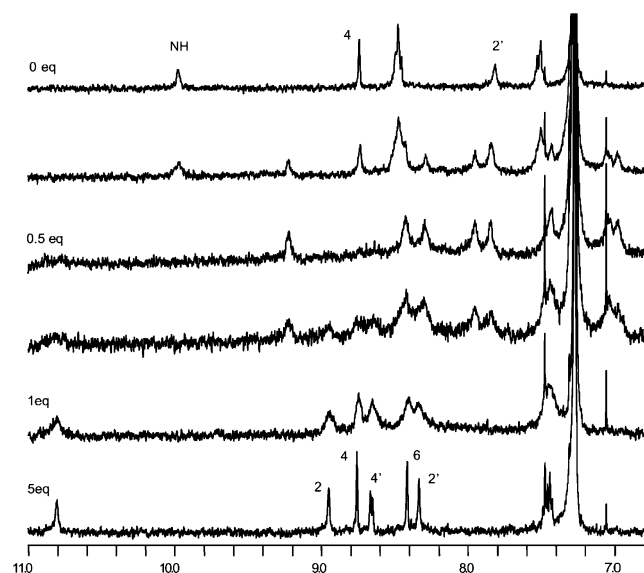
Figure 4. ^{1}H NMR (500 MHz) titration of **1a** with HSO_4^-. The macrocycle and its 2:1 and 1:1 anion complexes are in slow equilibrium on the NMR time scale ([**1a**] = 0.5 mM in 2% DMSO-d_6/CDCl$_3$). All spectra were recorded at 296 K.

and could not be detected above 1.0 equiv of added anion. Although both HSO_4^- and $H_2PO_4^-$ have symmetrical charge distributions and induced the formation of the 2:1 complexes with **1**, their 1:1 complexes showed chemical shift changes more similar to those observed in the *p*-TsO$^-$ complex than in the halide anion complex. The NH, C2H, and C2′H proton signals showed large downfield shifts with little or no change in the other resonances. Although it was difficult to assign the second set of signals, which are broad because of chemical exchange, it is clear that several protons in the macrocycle shifted upfield on formation of the 2:1 complex, as with halide anions.

The predominant formation of only one type of complex in the presence of 0.5 and 1.0 equiv of anion substrate indicates that the association constants K_1 and K_2 are relatively large compared with $1/[M]_t$ ($[M]_t$: total concentration of the macrocycle) and the ratio between them (K_2/K_1) is small. Although it is difficult to use ^{1}H NMR spectrometry to determine the concentrations of all the macrocyclic species in a mixed equilibrium with large association constants, minimum values of K_1 and K_2 could be estimated using the following method. Mole fractions of the macrocyclic species in the equilibria should satisfy the following conditions, assuming that the ^{1}H NMR signals of a minor species whose mole fraction (*f*) is less than 0.1 (0.05 for M$_2$I) are too weak to be detected in the spectrum of the complex mixture.

$$f_M, f_{MI} < 0.1 \qquad \text{when } [I]_t = [M]_t/2$$

$$f_M, 2f_{M2I} < 0.1 \qquad \text{when } [I]_t = [M]_t$$

where $[I]_t$ is the total concentration of the ion. One can derive the following equation for [M] as a function of [I] and $[M]_t$ from the equilibrium constant equations ($K_1 = [MI]/([M][I])$ and $K_2 = [M_2I]/([MI][I])$).

$$[MI] = \frac{\sqrt{(1 + K_1[I])^2 + 8K_1K_2[M]_t[I]} - (1 + K_1[I])}{4K_1K_2[I]}$$

$$[MI] = K_1[M][I]$$

$$[M_2I] = K_1K_2[M]^2[I]$$

[M] was calculated for a series of values of [I] with initial estimates of K_1 and K_2. Each result was used to calculate [MI] and [M$_2$I] and then the mole fractions of each macrocyclic species. It was found that K_1 and K_2 should be equal to or greater than 3×10^7 and 9×10^4 M^{-1}, respectively, to satisfy the above conditions (Figure 5). If K_1 is lower than this minimum value, a significant amount of M$_2$I would be present in the equilibrium mixture with 1 equiv of the anion (Figure 5b). If K_2 is lower than the minimum estimate, M and MI would exist in large quantities in the mixture with 0.5 equiv of the anion (Figure 5c). Not only the absolute values of K_1 and K_2 but also their ratio is important to satisfy the experimental data. The value of K_2/K_1 should be equal to or less than 0.003 to fulfill the above conditions. If the ratio is greater than 0.003, a significant amount of M$_2$I would be present in a 1:1 mixture of **1** and the anion (Figure 5d).

Anion Binding in Polar Solvents. The interaction between macrocycle **1** and anion substrates was significantly weaker in more competitive hydrogen bonding solvents. When the amount of DMSO-d_6 was increased, the association constants and $\Delta\delta$ values decreased. The effect was so great with halide and nitrate anions that M$_2$I complex formation could not be observed in 50% DMSO-d_6/CDCl$_3$. However, tetrahedral anions such as *p*-TsO$^-$, HSO$_4^-$, and H$_2$PO$_4^-$ retained strong binding in neat DMSO-d_6 with the H$_2$PO$_4^-$ complex still showing slow exchange on the NMR time scale (Figure 6). In DMSO-d_6, the chemical shift changes fit well into the 1:1 binding model and the NH, C2H, C2′H, and C4′H protons shifted downfield upon anion binding. The $\Delta\delta$ of the amide NH proton was relatively small for the HSO$_4^-$ and *p*-TsO$^-$ complexes (less than +0.2 ppm) but large for the H$_2$PO$_4^-$ complex (+1.62 ppm) presumably because of the higher basicity of the phosphate anion.

Convergent Hydrogen Bonding: Control Experiments. An acyclic analogue of **1** was synthesized and tested for anion binding in order to study the importance of binding site preorganizaton (Figure 7). Control **10**, assembled from **5**, aniline, and benzoyl chloride, has three amide bonds, each with two aryl substituents, and can be considered as a ring-opened form of macrocycle **1a**, with the same number and type of hydrogen bond donors. Although the molecule produces a more complex ^{1}H NMR spectrum because of its lack of symmetry, the proton signals could be assigned using the same 2D NMR techniques employed for the assignment of the macrocycle spectrum. First, the protons attached to the same phenyl ring were grouped together using a COSY45 experiment in which two protons in ortho or meta positions with each other are correlated by corresponding cross-peaks. Each proton was then assigned specifically using one or more NOEs between the adjacent protons (NH−C2H, NH−C2′H, C2H−C2′H, and C6H−C6′H). In the control molecule, additional NOEs were observed between NH−C4H, NH−C4′H, C2H−C6′H, and C6H−C2′H protons.

Comparison of the proton chemical shifts of macrocycle **1a** and acyclic analogue **10** provides insights into the effect of macrocyclization on the molecular conformation. The C2H, C6H, C5′H, and C6′H protons of both molecules have similar
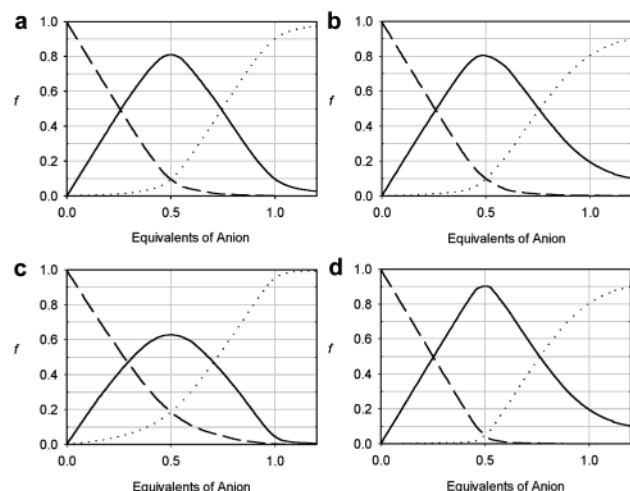
Figure 5. Theoretical mole fractions of the macrocyclic species in a mixed equilibrium, with $[M]_t = 0.5$ mM: f_M, dashed line; f_{MI}, dotted line; $2f_{M2I}$, solid line. (a) $K_1 = 3.0 \times 10^7$ M^{-1}, $K_2 = 9.0 \times 10^4$ M^{-1}; (b) $K_1 = 6.0 \times 10^6$ M^{-1}, $K_2 = 9.0 \times 10^4$ M^{-1}; (c) $K_1 = 3.0 \times 10^7$ M^{-1}, $K_2 = 1.8 \times 10^4$ M^{-1}; (d) $K_1 = 3.0 \times 10^7$ M^{-1}, $K_2 = 4.5 \times 10^5$ M^{-1}.
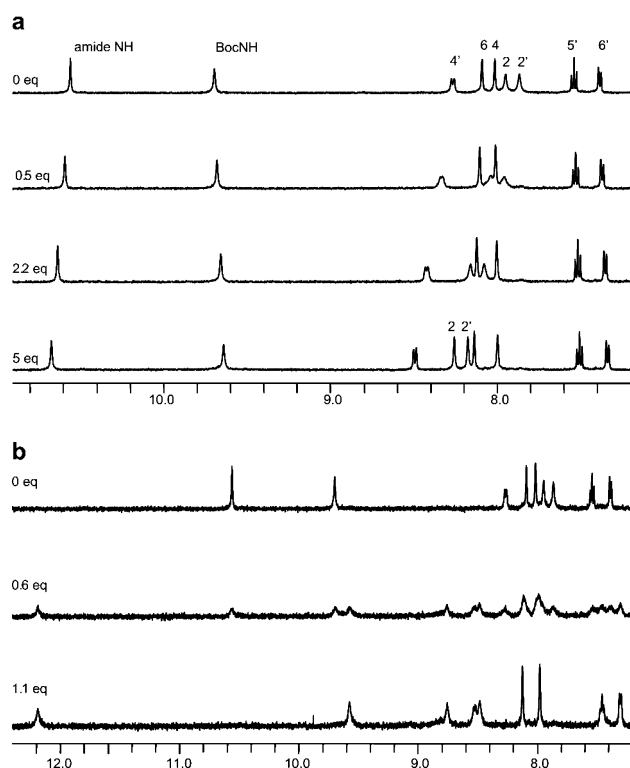

Figure 6. Titration of **1b** (1.0 mM in DMSO-d_6) at 296 K (a) with HSO$_4^-$. In this polar solvent, 2:1 complex formation was not observed and the 1:1 complex ($K_a = 1.7 \times 10^3$ M^{-1}) is in a fast equilibrium with the free macrocycle. (b) With H$_2$PO$_4^-$. The 1:1 complex ($K_a = 1.5 \times 10^4$ M^{-1}) still shows slow exchange on the NMR time scale (500 MHz ^{1}H frequency).

chemical shifts. Compared to **10**, the macrocycle C2′H proton peak is located more than 0.20 ppm upfield and the C4H and C4′H proton peaks are moved downfield by more than 0.15 and 0.55 ppm, respectively. The major conformational difference between the two molecules is the relative orientations of the amide groups, which are constrained convergently in the macrocycle. The large difference in the C4′H chemical shifts of **1a** and **10** reflects the rigid arrangement of the amide groups in the macrocycle, which enforces proximity of the carbonyl oxygen atom and the C4′H proton.
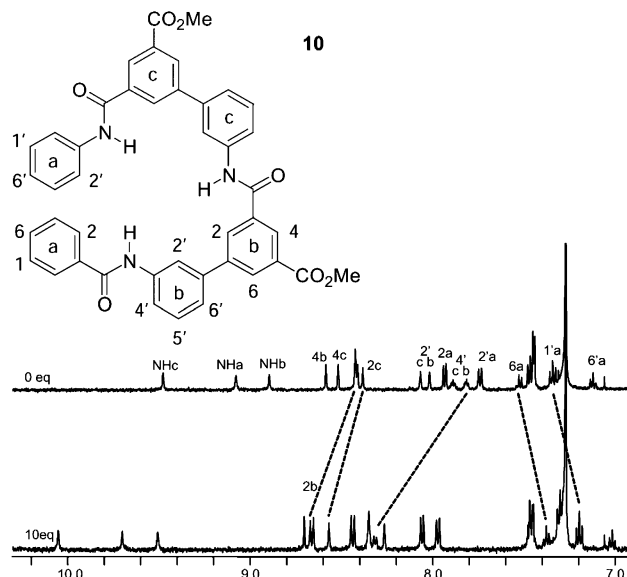
Figure 7. Titration of acyclic control **10** (0.5 mM in 2% DMSO-d_6/CDCl$_3$) with NO$_3^-$.

NMR titration experiments with **10** were carried out under the same conditions used for the macrocycles, and the observed chemical shift changes fitted well to a 1:1 binding model. The C6H, C5′H, and C6′H protons of the biphenyl units showed little chemical shift changes during the titration experiments, while the NH, C2H, and C2′H proton signals shifted downfield significantly, indicating that the acyclic molecule binds anions in a manner similar to that of the macrocycle. The downfield shifts of the C4H and C4′H protons can be ascribed to the conformational change that occurs in the acyclic triamide as it wraps around the anion in the complex. As a result, the amide protons are projected inward and the carbonyl oxygen atoms are positioned close to the C4H and C4′H protons, resembling the conformation of the macrocycle. Acyclic **10** showed much weaker binding to all anions tested, confirming that the rigid display of functional groups in a preorganized binding site makes a large positive contribution to the binding energy (Table 1).

The importance of convergent hydrogen bonds in anion recognition was also demonstrated by the complete loss of anion binding ability in DMSO of macrocycle **11**,[11] which has two imidazole rings in place of the phenyl rings in **1** (Figure 8a). The 2D NMR experiments clearly showed that 1-*H*-imidazole is the tautomeric configuration of the imidazole rings within macrocycle **11**, presumably due to hydrogen bonding between the amide protons and adjacent imidazole nitrogen atoms. The partial positive charge of the amide proton is masked by the partial negative charge of the imidazole N3 nitrogen atom, as indicated by semiempirical calculations (Figure 8b). As a result, the amide protons participating in an intramolecular hydrogen bond are not available for intermolecular interactions and the anion titration experiments with macrocycle **11** in DMSO-d_6 showed no spectral changes, indicating neither anion binding nor tautomerization.

Conclusion: Selective Anion Binding

Macrocycle **1** possesses size-selective anion recognition properties because I$^-$ showed much higher binding affinity than

---

(11) The synthesis and characterization of macrocycle **11** are described in the Supporting Information.
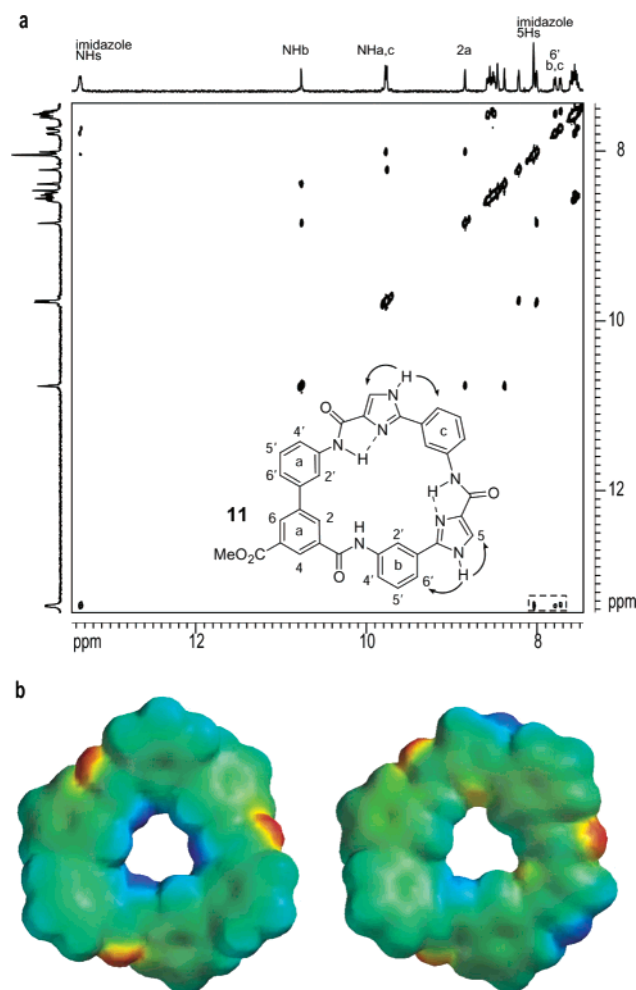
Figure 8. (a) NOESY spectrum of macrocycle **11** in DMSO-d_6. NOEs were observed between imidazole NH protons and their neighboring C5 and C6′. Two imidazole 5H proton signals overlap each other. The mixing time was set as 0.8 s with 500 MHz ^{1}H NMR frequency. (b) Electrostatic potential plots of macrocycle surfaces. The central cavity of macrocycle **1** (left) is lined with protons with partial positive charge. The cavity of macrocycle **11** (right) is almost charge-neutral. The partial positive charge of the amide protons is masked by the partial negative charge of the imidazole nitrogen atoms. Functional groups on the periphery of the macrocycle were omitted in the calculation, which was performed using the semiempirical AM1 model (PC Spartan Pro, release 6.0.6). Calculated molecular surfaces were colored according to electrostatic potential (blue, positive; red, negative).

Cl$^-$ (Table 1), which nonetheless has higher charge density. This selectivity can be explained by the large size and rigidity of the binding site. The rigid macrocyclic scaffold cannot undergo conformational adjustment to accommodate a variety of substrate sizes. The $\Delta\delta$ values of the interior protons in the macrocycle are sensitive to the shape of the bound anion. While the tetrahedral anion complexes showed a large $\Delta\delta$ (greater than +0.8 ppm) of the amide proton in 2%DMSO-d_6/CDCl$_3$, the other anion complexes showed small or negative $\Delta\delta$ (−0.35 to +0.05 ppm). In addition, the relative ratio between $\Delta\delta$ of C2′H and C2H ($\Delta\delta2'/\Delta\delta2$) was much larger for the planar (3.0) and spherical (2.2~2.8) anion complexes than the tetrahedral anion complexes (1.1−1.2), indicating a different binding mode for the different anions (Figure 2b vs Figure 3a). The distances and relative orientations of the macrocycle protons and the charged substrates depend on the size and shape of the anion. For

Table 1. Association Constants (M^{-1}) of **1** and **10** with Tetrabutylammonium Salts at 296 K^a

| anion | **1a**^{b} | **1b** in DMSO-d_6 | | | **10** |
		2%^{b}	50%^{c}	100%^{d}	
I$^-$	1.3×10^5	1.2×10^5	<10	<10	120^b
	(1.1×10^4)	(9.0×10^3)			
Cl$^-$	8.8×10^3	7.6×10^3	<10	<10	e
	(1.7×10^3)	(1.9×10^3)			
NO$_3^-$	4.6×10^5	e	110	20	620^b
	(2.1×10^3)				
p-TsO$^-$	2.6×10^5	2.1×10^5	3.3×10^3	780	e
HSO$_4^-$	f	f	7.5×10^3	1.7×10^3	e
H$_2$PO$_4^-$	f	f	e	$1.5 \times 10^{4\ g}$	500^d

^{a} Determined by titrating 0.5−1.0 mM macrocycle solution with salt solution. The salt solution contains the macrocycle at its initial concentration to account for dilution effects. The association constant of the 2:1 complex (K_2) is included in parentheses when applicable. Owing to the directionality of macrocycle **1**, two diastereomers of the 2:1 complex could be formed: parallel and antiparallel isomers. However, only a single isomer formation was assumed for the association constant calculation. This assumption is supported by the observation of only a single set of ^{1}H signals for the 2:1 complex under slow exchange conditions. Estimated errors are within ±20%. ^{b} In 2% DMSO-d_6/CDCl$_3$. ^{c} In 50% DMSO-d_6/CDCl$_3$. ^{d} In DMSO-d_6. ^{e} Not determined. ^{f} Slow equilibrium among free macrocycle, 1:1 and 2:1 complexes were observed. The association constants were not calculated. ^{g} Slow equilibrium was observed.

example, the oxygen atoms of tetrahedral anions, where the negative charge is localized, will be positioned at similar distances from the C2′H and C2H protons in a macrocycle–anion complex (2.5 and 2.8 Å, respectively, for the calculated structure of the *p*-TsO$^-$ complex, Figure 2a). The difference becomes larger for the 1:1 complex with I$^-$ where the anion center is 3.3 Å away from C2′H and 4.3 Å from C2H (Figure 3c). According to this model, I$^-$ makes direct contact with the C2′H protons but not the amide protons. The hydrogen bond donating amide protons are located 3.5 Å from the center of the anion. The location of the amide protons at sterically congested corners of the macrocycle cavity requires tetrahedral arrangement of anion charge centers for simultaneous formation of three optimal hydrogen bonds. This geometrical requirement is fulfilled by sulfate and phosphate oxyanions, resulting in the selective recognition by the macrocycle.

In summary, the molecular recognition properties of a novel anion receptor based on the rigid disposition of hydrogen bonding groups in the interior of a macrocyclic scaffold have been characterized. Unlike other macrocycles widely used for molecular recognition studies, the modular stepwise synthesis of the cyclic trimer of 3′-amino-3-biphenylcarboxylic acid makes modifications inside the central cavity relatively straightforward. Furthermore, the convergent projection of dipoles enables the macrocycle to bind anions with size and shape selectivity.

Experimental Section

Materials and Methods. All chemicals used for synthesis were of reagent grade quality, obtained from Aldrich or Fisher and used without further purification. THF was freshly distilled from Na/benzophenon, and CH$_2$Cl$_2$ was freshly distilled from CaH$_2$. Other solvents used were of anhydrous grade quality purchased from Aldrich. Reactions requiring anhydrous conditions were performed under an atmosphere of dry N$_2$. Silica gel (60 Å) was used for all column chromatography and TLC. NMR spectra were recorded on Bruker AM500, DPX400, DPX500, and GE 300 spectrometers at room temperature unless otherwise stated, and chemical shifts are reported as ppm relative to internal TMS or residual solvent. Mass spectra were acquired at the University of Illinois Mass Spectrometry Center. Melting points were determined using an

electrothermal melting point apparatus (Fisher) and are uncorrected. Elemental analyses were performed at Atlantic Microlabs, Norcross, GA.

3,5-Dimethyl-3′-nitro-1,1′-biphenyl (2). 3-Nitrophenylboronic acid (3.65 g, 1.06 equiv) was dissolved in 50 mL of toluene/15 mL of EtOH. 3,5-Dimethyliodobenzene (3 mL, 20.6 mmol) and Na_2CO_3 solution (2 N in H_2O, 25 mL) were added and then followed by $Pd(Ph_3P)_4$ (0.80 g, 3.3 mol %). The reaction mixture was refluxed for 3 h and then allowed to cool to room temperature. The mixture was partitioned between ether and water. The organic layer was washed with saturated $NaHCO_3$ solution and brine and dried over anhydrous Na_2SO_4. After filtering off the solid, the solvent was removed by evaporation. The residue was purified by SiO_2 chromatography (hexane/EtOAc, 19:1) to give the product as a white solid (4.4 g, 94%): mp 68−70 °C; ^{1}H NMR (300 MHz, $CDCl_3$) δ 8.44 (m, 1H), 8.16−8.20 (m, $J^3 = 8.0$ Hz, 1H), 7.89−7.92 (m, $J^3 = 7.8$ Hz, 1H), 7.56−7.61 (m, 1H), 7.24 (s, 2H), 7.08 (s, 1H), 2.41 (s, 6H); HRMS (FAB) m/z 227.0945 (M^+, calcd for $C_{14}H_{13}NO_2$ 227.0945).

5-(Ethoxycarbonyl)-3′-nitro-1,1′-biphenyl-3-carboxylic Acid (3). Compound **2** (4.4 g, 19.3 mmol) was dissolved in 40 mL of pyridine/20 mL of H_2O by heating. $KMnO_4$ (24.8 g, 8 equiv) was added portionwise while the mixture was refluxing. The mixture was refluxed for an additional 6 h and then allowed to cool to room temperature. After overnight stirring, the mixture was filtered through a Celite pad and the filtrate was concentrated. A 1 N NaOH solution was added to the residue, and the undissolved material was removed by filtration. The filtrate was acidified with concentrated HCl in an ice/water bath and extracted with EtOAc (×3). Combined EtOAc layers were washed with 0.1 N HCl solution and brine and then dried over Na_2SO_4. The solvent was removed by evaporation and the residue was further dried under vacuum to give the crude dicarboxylic acid (4.57 g). This dicarboxylic acid and *p*-toluenesulfonic acid (0.30 g, 0.1 equiv) were dissolved in EtOH (300 mL). The mixture was refluxed overnight. After the solution was cooled, its volume was reduced to $^1/_3$ by evaporation. The residue was diluted with THF and washed with 5% $NaHCO_3$ solution and brine. The organic layer was dried over Na_2SO_4, and the solvent was removed by evaporation. The residue was purified by recrystallization (EtOAc/hexane) to give the diester (50%, two steps). This diester was dissolved in 60 mL of THF/20 mL of EtOH. To the solution, NaOH (1.0 equiv) in 20 mL of H_2O was added slowly, and the stirring was continued overnight. The mixture was extracted with ether, and the aqueous layer was acidified with 2 N HCl. The resulting mixture was extracted with CH_2Cl_2, and the organic layer was dried over Na_2SO_4. The solvent was removed by evaporation, and the residue was purified by SiO_2 chromatography (MeOH/CH_2Cl_2, 2:98) to give the product as a white solid (1.58 g, 52%): mp 190−192 °C; ^{1}H NMR (400 MHz, $CDCl_3$) δ 8.82 (m, 1H), 8.53−8.58 (m, 3H), 8.29−8.32 (m, $J^3 = 8.1$ Hz, 1H), 8.01−8.04 (m, $J^3 = 7.6$ Hz, 1H), 8.69−8.73 (m, 1H), 4.49 (q, $J = 7.1$ Hz, 2H), 1.47 (t, $J = 7.1$ Hz, 3H); ^{13}C NMR (100 MHz, $CDCl_3$) δ 169.14, 165.24, 148.87, 140.66, 139.65, 133.19, 133.09, 132.69, 132.26, 131.04, 130.60, 130.21, 123.13, 122.16, 61.87, 14.38; HRMS (FAB) m/z 338.0644 ([M + Na]$^+$, calcd for $C_{16}H_{13}NO_6$Na 338.0641).

Monomethyl 5-Bromoisophthalate (4). Monomethyl 5-nitroisophthalate was hydrogenated using MeOH as solvent. DMF was added to dissolve the product before filtration through a Celite pad. The product (1 g, 5.1 mmol) was dissolved in 15% aqueous HBr (22.5 mL), and the mixture was cooled in an ice bath. A 2.5 M aqueous $NaNO_2$ (2.3 mL, 1.1 equiv) solution was slowly added to generate the diazonium salt. CuBr (0.98 g, 1.3 equiv) was dissolved in 15% HBr (9 mL), and this mixture was cooled in an ice bath. The diazonium salt solution was added to CuBr solution, and the temperature was raised to room temperature. After 30 min, the mixture was heated to 70 °C and stirring was continued for an additional 1 h. After the mixture was cooled in an ice bath, the precipitate was collected by filtration and washed with water. The product was purified by passing through a short SiO_2 column

(MeOH/CH_2Cl_2) to give the product as white solid (1.26 g, 95%): mp 191−193 °C; ^{1}H NMR (500 MHz, DMSO-d_6) δ 8.41 (s, 1H), 8.27 (2H), 3.90 (s, 3H); HRMS (FAB) m/z 280.9427 ([M + Na]$^+$, calcd for $C_9H_7O_4$BrNa 280.9425).

5-(Methoxycarbonyl)-3′-nitro-1,1′-biphenyl-3-carboxylic Acid (5). Compound **4** (0.26 g, 1 mmol), 3-nitrophenylboronic acid (0.17 g, 1 equiv), and $Pd(OAc)_2$ (7 mg, 0.03 equiv) were dissolved in 4 mL of DMF, and the solution was degassed. A 1.5 M aqueous Cs_2CO_3 (2 mL, 3 equiv) solution was added, the mixture was heated to 45 °C, and the stirring was continued for 1.5 h. After the mixture was cooled to room temperature, 10 mL of H_2O was added and the solution was slightly acidified with 2 N HCl. The mixture was extracted with EtOAc/THF (1:1), and the organic layer was washed with brine and dried over Na_2SO_4. After the solid was filtered off, the solvent was removed by evaporation. The residue was purified by recrystallization (THF/hexane) to give the product as an off-white solid (0.24 g, 81%): mp 246−248 °C; ^{1}H NMR (400 MHz, DMSO-d_6) δ 8.52 (s, 1H), 8.51 (s, 1H), 8.48 (s, 1H), 8.47 (s, 1H), 8.30 (d, $J^3 = 8.2$ Hz, 1H), 8.25 (d, $J^3 = 7.8$ Hz, 1H), 7.79−7.83 (m, 1H), 3.94 (s, 3H); ^{13}C NMR (100 MHz, DMSO-d_6) δ 166.22, 165.33, 148.50, 139.81, 139.13, 133.77, 132.48, 132.13, 131.59, 131.15, 130.83, 129.53, 123.15, 121.76, 52.70; HRMS (FAB) m/z 324.0487 ([M + Na]$^+$, calcd for $C_{15}H_{11}NO_6$Na 324.0484).

3-[(*tert*-Butoxycarbonyl)amino]-5-iodobenzoic Acid (7). Compound **6**[12] (1.36 g, 4.6 mmol) was dissolved in 20 mL of concentrated NH_3/H_2O. To the solution, ammonium iron(II) sulfate hexahydrate (10.6 g, 5.8 equiv) in 20 mL of H_2O was added. After refluxing for 10 min, the mixture was filtered through a Celite pad and the filtrate was cooled in an ice/water bath. The pH was adjusted to ∼4 with concentrated HCl, and the mixture was extracted with EtOAc (×3). The combined organic layers were washed with brine and dried over Na_2SO_4. The solvent was removed by evaporation to give the aniline product (1.07 g, 88%). This aniline compound (0.94 g, 3.6 mmol) was dissolved in 4 mL of 1,4-dioxane and 4 mL of 2 N KOH/H_2O. To the solution, (Boc)$_2$O (1.58 g, 2.0 equiv) was added, and stirring was continued overnight. After removal of dioxane by evaporation, the mixture was diluted with 6 mL of 1 N KOH and washed with ether. The aqueous layer was cooled in an ice/water bath and neutralized with 6 N HCl. The precipitate was collected by filtration and dried under vacuum (1.04 g, 80%): ^{1}H NMR (500 MHz, DMSO-d_6) δ 13.2 (br s, 1H), 9.68 (s, 1H), 8.08 (s, 1H), 8.07 (s, 1H), 7.80 (s, 1H), 1.48 (s, 9H); ^{13}C NMR (100 MHz, DMSO-d_6) δ 165.83, 152.55, 141.18, 133.11, 130.98, 129.81, 118.11, 94.42, 79.87, 28.02; HRMS (FAB) m/z 385.9867 ([M + Na]$^+$, calcd for $C_{12}H_{14}NO_4$INa 385.9865).

5-[(*tert*-Butoxycarbonyl)amino]-3′-nitro-1,1′-biphenyl-3-carboxylic Acid (8). Compound **7** (0.97 g, 2.7 mmol) and 3-nitrophenylboronic acid (0.45 g, 1.0 equiv) were dissolved in 8 mL of DMF. To the solution, Na_2CO_3 solution (1.6 N in H_2O, 4 mL) was added and followed by $Pd(OAc)_2$ (18 mg, 3 mol %). The mixture was then stirred at 80 °C for 4 h, after which it was cooled to room temperature and 20 mL of H_2O was added. The mixture was acidified (pH ∼4) by adding 2 N HCl and then was extracted with EtOAc (×3). The combined organic layers were washed with brine and dried over Na_2SO_4. The solvent was removed by evaporation and the residue was purified by SiO_2 chromatography (MeOH/CH_2Cl_2, 4:96) to give the product as a white solid (0.79 g, 83%): mp 301−304 °C; ^{1}H NMR (500 MHz, DMSO-d_6) δ 9.72 (s, 1H), 8.37 (m, 1H), 8.25−8.27 (m, $J^3 = 8.2$ Hz, 1H), 8.19 (s, 1H), 8.10−8.12 (m, $J^3 = 7.8$ Hz, 1H), 8.05 (s, 1H), 7.86 (s, 1H), 7.78−7.81 (m, 1H), 1.50 (s, 9H); ^{13}C NMR (125 MHz, DMSO-d_6) δ 166.97, 152.83, 148.45, 140.97, 140.75, 138.66, 133.29, 132.37, 130.80, 122.70, 121.28, 121.13, 120.45, 118.78, 79.71, 28.10; HRMS (FAB) m/z 381.1064 ([M + Na]$^+$, calcd for $C_{18}H_{18}N_2O_6$Na 381.1063).

General Procedure for 2-(Trimethysilyl)ethyl Ester Synthesis. The carboxylic acid was dissolved in CH_2Cl_2/THF (4:1). To the solution,

(12) Auman, B. C.; Myers, T. L.; Highley, D. P. *J. Polym. Sci. A* **1997**, *35*, 2441−2451.

4-(dimethylamino)pyridine (0.2 equiv) and 2-(trimethylsilyl)ethanol (1.0 equiv) were added and followed by dicyclohexylcarbodiimide (1.0 equiv). The mixture was stirred overnight and filtered to remove the urea byproduct. The filtrate was evaporated and purified by SiO$_2$ chromatography (hexane/EtOAc).

General Procedure for 2-(Trimethysilyl)ethyl Ester Cleavage. The ester was dissolved in THF, and 1 M tetrabutylammonium fluoride/THF (3 equiv) was added. After 4 h, concentrated NH$_4$Cl was added and the mixture was diluted with EtOAc and washed with brine. The organic layer was dried over Na$_2$SO$_4$ and purified by SiO$_2$ chromatography (MeOH/CH$_2$Cl$_2$).

General Procedure for Nitro Group Hydrogenation. The nitro compound was dissolved in MeOH/EtOAc (1:1), 10% Pd/C was added to the solution, and the mixture was shaken under H$_2$ (40 psi) until the starting material disappeared on HPLC. The catalyst was removed by filtration. The solvent was evaporated, and the residue was dried under vacuum.

General Procedure for Amide Bond Formation. The carboxylic acid and aniline compounds were dissolved in THF. To the mixture, bis(2-oxo-3-oxazolidinyl)phosphinic chloride (1.2 equiv) and diisopropylethylamine (2.5 equiv) were added, and stirring was continued overnight. The mixture was diluted with EtOAc and washed with saturated NaHCO$_3$ and brine. The organic layer was dried over Na$_2$SO$_4$ and purified by SiO$_2$ chromatography (hexane/EtOAc). The cyclization of the linear trimer with the same procedure under dilute condition (1 mM) gave the macrocycle in 40−60% yields.

5-*tert*-Butoxycarbonylamino-3′-[(5-*tert*-butoxycarbonylamino-3′-nitrobiphenyl-3-carbonyl)amino]biphenyl-3-carboxylic Acid 2-Trimethylsilanylethyl Ester (9, R = NHBoc). Mp 161 °C; ^{1}H NMR (400 MHz, CDCl$_3$) δ 8.44 (s, 1H), 8.41 (s, 1H), 8.19 (d, J^3 = 8.2 Hz, 1H), 7.87−7.93 (m, 5H), 7.85 (s, 1H), 7.79−7.82 (m, 2H), 7.71 (s, 1H), 7.55−7.60 (m, 1H), 7.37−7.41 (m, 1H), 7.34 (d, J^3 = 7.7 Hz, 1H), 7.04 (s, 1H), 6.83 (s, 1H), 4.38−4.42 (m, 2H), 1.54 (s, 9H), 1.53 (s, 9H), 1.11−1.15 (m, 2H), 0.08 (s, 9H); ^{13}C NMR (100 MHz, CDCl$_3$) δ 166.42, 165.19, 152.81, 152.79, 148.59, 141.63, 141.55, 140.73, 140.08, 139.75, 138.97, 138.26, 136.48, 133.25, 131.78, 129.85, 129.54, 123.51, 122.77, 122.62, 121.96, 121.34, 120.51, 120.12, 120.00, 119.09, 118.42, 116.88, 81.31, 80.99, 63.58, 28.32, 28.31, 17.45, −1.45; HRMS (FAB) m/z 791.3085 ([M + Na]$^+$, calcd for C$_{41}$H$_{48}$N$_4$O$_9$NaSi 791.3088).

Macrocycle 1a. ^{1}H NMR (400 MHz, 5% DMSO-d_6/CDCl$_3$) δ 10.17 (s, 3H), 8.69 (s, 3H), 8.48 (s, 3H), 8.42−8.44 (m, 6H), 7.75 (s, 3H), 7.44−7.50 (m, 6H), 4.37 (q, J = 7.1, 6H), 1.37 (t, J = 7.1, 9H); ^{13}C NMR (100 MHz, 5% DMSO-d_6/CDCl$_3$) δ 165.25, 164.60, 140.16, 139.01, 138.88, 135.21, 131.40, 130.18, 129.40, 128.68, 128.38, 122.37, 120.37, 118.20, 60.89, 13.79; MS (FAB) m/z 824 [M + Na]$^+$, 840 [M + K]$^+$. Anal. Calcd for C$_{48}$H$_{39}$N$_3$O$_9$·H$_2$O: C, 70.32; H, 5.04; N, 5.13. Found: C, 70.10; H, 4.98; N, 5.15.

Macrocycle 1b. ^{1}H NMR (500 MHz, DMSO-d_6) δ 10.56 (s, 3H), 9.70 (s, 3H), 8.26 (d, J^3 = 7.9 Hz, 3H), 8.09 (s, 3H), 8.01 (s, 3H), 7.95 (s, 3H), 7.87 (s, 3H), 7.52−7.56 (m, 3H), 7.38 (d, J^3 = 7.9 Hz, 3H), 1.52 (s, 27H); ^{13}C NMR (125 MHz, DMSO-d_6) δ 165.56, 152.88, 140.64, 140.43, 140.21, 139.62, 136.21, 129.65, 122.35, 120.47, 119.45, 119.30, 119.05, 117.21, 79.56, 28.15; MS (FAB) m/z 953 [M + Na]$^+$, 969 [M + K]$^+$. Anal. Calcd for C$_{54}$H$_{54}$N$_6$O$_9$·H$_2$O: C, 68.34; H, 5.95; N, 8.86. Found: C, 68.17; H, 6.22; N, 8.63.

Supporting Information Available: Synthetic schemes and procedures for macrocycle **11**. This material is available free of charge via the Internet at http://pubs.acs.org.

JA034563X